HEALTH STATUS PREDICTION USING FTIR MICROSPECTROSCOPY OF BLOOD COMPONENTS AND CLUSTER ANALYSIS

Jacov Mordehai[1], Jagannathan Ramesh[2], Mahmoud Huleihel[3], Zahavi Cohen[1], Oleg Kleiner[1], Marina Talyshinsky[3], Vitaly Erukhimovitch[3], Aviv Cahana[2] and Shaul Mordechai[2*]

[1]Department of Pediatric Surgery, Soroka University Medical Center, Ben Gurion University, Beer Sheva 84101, Israel.

[2]Department of Physics, Ben Gurion University, Beer Sheva 84105, Israel.

[3]The Institute for Applied Biosciences, Ben Gurion University, Beer Sheva 84105, Israel.

* denotes the corresponding author

Tel : +972-8-646 1749 ; Fax : +972-8-647 2903

E-mail : shaulm@bgumail.bgu.ac.il

Running title : Health status prediction by novel optical technology

Keywords : FTIR-microspectroscopy ; Blood ; Infection; WBC ; Plasma ; Cluster analysis

Abstract

Background : FTIR spectroscopy has been widely applied in biology and recently also in medicine. Biophysicists apply FTIR to characterize the structure and conformation of biomolecules. With the introduction of microscopy to the FTIR setup, applications in medicine have become a reality. Diagnosis of various types of malignancies such as lung, breast and colon cancers is already reported in the literature. FTIR has also been used to analyze the body fluids for the purpose of diagnostic and characterization. This study presents a novel methodology for the prediction of health status using FTIR data on blood components and cluster analysis. This is the first report in the field of optical diagnosis displaying the potential of FTIR-MC in the health care.

Methods : Blood samples were collected from thirty age-matched healthy controls and seven patients suffering due to various infections. Blood components such as WBC, RBC and plasma were isolated using standard procedures. FTIR-microspectroscopy of the blood components was performed and later cluster analysis of FTIR spectra was done using OPUS software.

Results : Differences were observed in absorbance and spectral patterns between the three blood components. FTIR spectra of WBC showed specific pattern changes in the case of patients suffering due to infection in comparison to the controls. Combination of FTIR-MC and cluster analysis could provide 100% classification between patients and healthy controls.

Conclusions : FTIR-MC can distinguish three components of blood using spectral variations and cluster analysis. Specific spectral changes were observed between infected patients and age-matched healthy controls. Cluster analysis of spectra of WBC provided good classification between patients and healthy controls.

Abbreviations

WBC : White Blood cells

RBC : Red Blood cells

FTIR-MC : Fourier Transform InfraRed MiCrospectroscopy

SUMC : Soroka University Medical Center

MCT : Mercury Cadmium Telluride

DNA : Deoxyribo Nucleic Acid

RNA : RiboNucleic Acid

1. Introduction

FTIR spectroscopy has a unique place in the area of spectroscopy as a powerful tool to characterize the inorganic and organic compounds by chemists [1]. Its application in biology for studying the structure and conformation of proteins [2], nucleic acids [3] and lipids [4] has been well documented in the literature. The advances made in the instrumentation such as the introduction of IR microscopy have paved the way to its usefulness in medicine [5]. FTIR Microspectroscopy (FTIR-MC) has been used to characterize various types of malignancies and other disorders. The main purpose of these reports was to explore the possibility of FTIR-MC for the early diagnosis of malignancies. Initial success in the diagnosis of different types of cancer such as lung [6], colon [7], breast [8] and cervix [9] have been reported.

Besides the application of FTIR to the tissue diagnostics, its role in the diagnostic aspects involving body fluids is gaining importance in the last few years. Mantsch group reported the successful diagnosis of arthritis based on NIR (Near InfraRed) analysis of synovial fluid obtained from the patients [10]. Mid-IR was shown to be useful in the identification of disease pattern using FTIR spectrum of human sera [11]. Quantification of serum components such as glucose, total protein, cholesterol and urea was achieved using FTIR spectroscopy [12]. Measurements of concentrations of urea, glucose, protein and ketone in human urine have been performed using NIR spectroscopy [13]. In this report, we present FTIR-MC spectra of blood components (serum, WBC and RBC) obtained from patients suffering due to infections and other hematological disorders. The subsequent cluster analysis of the FTIR-MC spectra showed that the identification of

"abnormality" could be achieved. Our preliminary data indicated that the deviation from normal health condition, which may be reflected in the blood, could be sensed by this technique with high reliability.

2. Materials and Methods

2.1 Clinical Methods

Blood samples were collected from patients and normal population (30 controls) with their consents in the age group between 1-18 years, admitted to the Department of Pediatric surgery, Soroka University Medical Center (SUMC). The blood samples were processed within two hours of collection. Procedure for the isolation of various components of blood was followed as reported earlier in the literature [14]. The undiluted blood components (WBC, RBC and plasma) were loaded on the zinc-sellinide crystals and air dried for four hours at 25 C in the laminar flow.

2.2 FTIR Microspectroscopy

FTIR measurements were conducted in transmission mode using the FTIR microscope IRscope II with sensitive MCT detector (BRUKER EQUINOX model 55/S OPUS software). The wavenumber range of the measured spectra was 600-4000 cm^{-1}. During each measurement, the measured sites were circular of about 100 μm diameter covering the component of interest in the sample. Such area contains enough quantity of sample to obtain good quality spectra with high signal to noise ratio. The spectra taken were average of 128/256 scans to increase the signal to noise ratio. Baseline correction for all the spectra were done using rubber band baseline correction method and the

spectra was amide I normalized after baseline correction for the entire spectrum. For each sample, the spectrum was taken as the average of ten different measurements. The signal to noise ratio was calculated for all the measurements and only the spectra with high signal to noise ratio (≥1000) were used for further data analysis.

2.3 Cluster Analysis

Cluster analysis was performed with good quality spectra having high signal to noise ratio. Baseline corrected and amide I normalized spectra were used for the analysis. The spectra of various blood components collected from ten different healthy controls were used. Different segments of FTIR spectra were analyzed in the analysis. In the case of infectious cases, seven patients suffering due to different infections were taken for study along with ten healthy controls. The Ward's minimum variance method which was provided in the OPUS software was used for the cluster analysis.

3. Results and Discussion

In order to achieve health status prediction, it is important to study and understand the blood components in terms of biomolecular changes using FTIR-MC. FTIR-microscopic spectra of the major blood components isolated from 10 controls (normal population), which include WBC, RBC and plasma, are presented in Figures 1-2. Representative spectra from 30 controls are shown in Figure 1. There was very good agreement among different controls as the standard deviation measured for the samples was small for all the three blood components. All the spectra shown in Figures 1-2 were

normalized to amide I peak at 1643 cm^{-1}. There were significant spectral differences between the three blood components. The expanded region given in Figure 2 shows the average of ten controls for WBC, RBC and plasma. Symmetric and asymmetric stretching vibrations from the phosphate group are seen in the FTIR spectra in the region between 950-1250 cm^{-1}. Apart from phospholipids, energy metabolites and phosphorylated proteins, nucleic acids are the main contributors of these bands in the cells. FTIR spectra of WBC showed clear bands at 965, 1080 and 1245 cm^{-1}, which were absent in RBC and plasma. WBC is composed of mononuclear cells containing nucleic acids such as DNA and RNA. The nucleic acid components are absent in RBC and plasma. In addition, the integrated absorbance measured for the three components showed that WBC had higher phosphate content than the other two components. The FTIR spectra of plasma showed a new peak at 1404 and around 1585 cm^{-1} which were absent in WBC and RBC components. The IR bands at 1404 and 1585 cm^{-1} could arise due to urea/triglycerides, which are abundant in the plasma compared to other two components. A small IR band at 1740 cm^{-1} was observed in the case of WBC (see Figure 1), which is an indication of cell death as reported in the literature [15].

FTIR-MC spectra of all three components in the higher wavenumber region between 2600-3600 cm^{-1} are shown in Figure 3. The absorbance of multiple bands between 2800-3000 cm^{-1} was higher for WBC than RBC and plasma. Asymmetric stretching vibrations of CH_2 and CH_3 from proteins, nucleic acids and phospholipids mainly contribute to this region of the spectrum. Hence, the higher absorbance for WBC in this region might be due to the nucleic acids content of the mononuclear cells. There

were significant spectral pattern changes observed for RBC and plasma components of the blood. Firstly, a small shoulder in the multiplet between 2800-3000 cm^{-1} disappeared in the case of RBC and plasma, which might be possibly due to the absence of certain biomolecular components. The ratio of the IR bands I to II shown in Figure 3 indicated that it followed the trend, WBC<1, RBC>1 and plasma=1 which could be observed for all the 10 controls reported in this study. The second derivative spectra of WBC (blue), RBC (red) and plasma (black) are shown in Figure 4. Significant frequency shifts were observed in the 1000-1300 cm^{-1} range for WBC with respect to the other two components. The plasma showed dramatic frequency shift near 1404 cm^{-1} compared to WBC and RBC components of the blood. IR band at 2923 showed a frequency shift for WBC in comparison to RBC and plasma components. The biomolecular differences among these three components are mainly responsible for the observed frequency shifts.

FTIR-MC spectra of all three blood components from patients suffered due to different infectious diseases are shown in Figures 5-6. Figure 5 shows the FTIR-MC spectra of WBC, RBC and plasma for two patients with acute appendicitis. Three age-matched controls are included for comparison with the infectious cases. Among the three components, significant spectral changes were observed in WBC especially in the phosphate-absorbing region (1000-1200 cm^{-1}) of the spectrum (Figure 5a). The absorbance of the infected was higher than the controls. The expanded region (see inlet in Figure 5a) of the spectra of WBC arising from phosphate group showed clear spectral pattern changes for the patients compared to the controls. Absence of any major spectral changes with RBC and plasma (Figure 5 b-c) is a clear indication that acute appendicitis,

which is caused by infection [16] leads to the triggering of the immune system. The immunological reaction involves the activation of T and B lymphocytes by series of phosphorylation of members of signal transduction cascade [17].

Figure 6 shows the FTIR-MC spectra of WBC, RBC and plasma isolated from the peripheral blood of a patient having infection in the armpit (axilla) as diagnosed by the physician. As observed in the case of acute appendicitis, the spectrum of WBC (Figure 6a and the inlet in the region 950-1280 cm^{-1}), the patient showed higher absorbance in the region of phosphate and similar spectral pattern changes. Other components such as RBC and plasma showed no notable spectral differences compared to controls.

Hierarchical cluster analysis is a simple method, which is used for classification purposes in medicine [18]. It is based on the distance between the nearest neighbors in a given cluster as it is presented in the dendrogram [19]. Dendrograms derived from cluster analysis of FTIR-MC spectra of the three components of the blood such as WBC, RBC and plasma isolated from ten different healthy controls are shown in Figure 7 a-c. Cluster analysis of the spectra in the symmetric stretching region of the phosphate group [20] showed two major clusters with high heterogeneity. One major cluster had two sub-clusters comprising plasma and RBC with relatively good classification accuracy. All the WBC samples were classified as a separate cluster. When the analysis was performed in the asymmetric stretching region of the phosphate as shown in Figure 7b, the results were similar to Figure 7a. The heterogeneity between the two sub-clusters having plasma and

RBC was lower compared with the results shown in Figure 7a. The cluster analysis of the region arising due to bending vibrations of CH_2 and CH_3 groups in proteins is shown in Figure 7c. Both RBC and WBC were classified as a major cluster, leaving the plasma as a separate cluster. Again, the heterogeneity between the two major and sub-clusters was high giving rise to good classification of all three-blood components. It can be understood that the presence of nucleic acids in WBC was responsible for the classification as a separate major cluster with symmetric and asymmetric stretching regions of the phosphate group. It is interesting to note that the major bimolecular components of RBC and plasma are proteins, which formed a second major cluster. In addition, the difference in the composition of phosphorylated proteins may account for the classification of RBC and plasma as two sub-clusters.

As the advances made by FTIR in medicine has been rising, our group present the novel approach to screen the general population for the possibility of infectious diseases. This approach combines both FTIR and cluster analysis of various blood components isolated from age-matched population. Figure 8 shows the dendrogram obtained from the cluster analysis of FTIR-MC spectra of WBC from age-matched controls and patients suffering due to variety of infections, which include five bacterial, and two viral infections. Analysis of the spectral region covering both symmetric and asymmetric stretching regions of the phosphate shown in Figure 8a classified controls and patients as two major clusters with reasonably good heterogeneity. In addition, the cluster analysis of narrow range of symmetric stretching region of phosphate showed similar results to the inclusion of both regions. The cluster analysis of FTIR-MC spectra of plasma isolated

from controls and infected patients was also performed. The results as shown in Figure 8c showed major and minor clusters, where the mixing of both controls and patients was observed. The plasma component of the blood could not provide accurate classification of controls and infected patients. This might be due to the direct involvement of WBC on exposure to infections and subsequent biomolecular changes compared to the plasma in the blood.

To evaluate the validity of the method, a blind test was performed with four unknown cases provided by the expert physician. Results of the test are presented in Figure 9 a-b. Cluster analysis of WBC spectra in the 945-1282 (comprises both symmetric and asymmetric regions of phosphate) and 1146-1282 cm^{-1} provided similar results. Our predictions matched with the physician's diagnosis with 100% accuracy. As per the physician, TST 1, 3, 4 were healthy controls and TST 2 was an infected patient. It is interesting to realize that our method of classification had high sensitivity and specificity. These preliminary results are yet to be confirmed with larger number of cases. Modern clinical methods do offer accurate diagnosis of infections [21,22] stating the exact cause of infection. This report is the first of the kind showing the application of FTIR-MC in defining health status with specific reference to infections. Our results are encouraging and further research is required to explore the usefulness of this approach to other branches of medicine.

4. Conclusions

FTIR-microspectroscopy studies showed significant differences in the spectral features between the three major components of the blood obtained from controls. Phosphate absorbing regions of the spectra exhibited notable changes in absorbance for WBC compared to the other two components. Cluster analysis showed good classification of all three components with high heterogeneity. The FTIR-MC spectra of WBC showed specific pattern changes in the phosphate absorbing region between infected patients and age-matched healthy controls. Cluster analysis of WBC spectra classified patients and controls with 100% accuracy. Preliminary blind tests conducted in this study provided correct classification of all the test cases using combination of FTIR-MC spectra of WBC and cluster analysis. Extensive studies in this direction are required for the application of this approach to other disorders in the future.

Acknowledgements

This research work was supported by the Israel Science Foundation (ISF Grant No : 788/ 01), the Harry Stern Applied Research Grant Program and the research grant from the Faculty of Health at Ben Gurion University of the Negev received by Dr. Jacov Mordehai during the course of this work. Many thanks are due to Dr. B. Cohen for fruitful discussions.

References

1. Roeges NPG, A Guide to the complete interpretation of infrared spectra of organic structures, UK : John Wiley & Sons, 1994

2. Cooper EA, Knutson K. Fourier transform infrared spectroscopy investigation of protein structure. Pharm Biotechnol 1995 ; 7 : 101-143

3. Mantsch HH, Chapman D, Infrared spectroscopy of biomolecules, New York : Wiley-Liss, 1996.

4. Brandenburg K, Seydel U. Infrared spectroscopy of glycolipids. Chem Phys Lipids 1998 ; 96 : 23-40.

5. Diem M, Boydston-White S, Chiriboga L. Infrared spectroscopy of cells and tissues: Shining light onto a novel subject. Applied Spectroscopy 1999 ; 53 : 148-161.

6. Wang HP, Wang HC, Huang YJ. Microscopic FTIR studies of lung cancer cells in pleural fluid. Sci Total Environ 1997 ; 204 : 283-287.

7. Argov S, Ramesh J, Salman A, Igor S, Goldstein J, Guterman H, Mordechai S. Diagnostic potential of FTIR Microspectroscopy and advanced

computational methods in colon cancer patients. J. Biomed. Opt 2002 ; 7 : 1-7.

8. Dukor RK, Liebman MN, Johnson B. A new non-destructive method for analysis of clinical samples with FTIR-microspectroscopy. Breast cancer as an example. Cell. Mol. Biol 1998 ; 44 : 211-217.

9. Cohenford MA, Rigas B. Cytologically normal cells from neoplastic cervical samples display extensive structural abnormalities on IR spectroscopy : implications for tumor biology. Proc. Natl. Acad. Sci USA. 1998 ; 95 : 15327-15332.

10. Shaw RA, Kotowich S, Eysel HH, Jackson M, Thomson GT, Mantsch HH. Arthritis diagnosis based upon the near-infrared spectrum of synovial fluid. Rheumatol Int 1995 ; 15 : 159-165.

11. Petrich W, Dolenko B, Früh J et.al Recognition of disease-specific patterns in FT-IR spectra of human sera. Proceedings of SPIE 2000 ; 3918 : 91-96.

12. Shaw RA, Kotowich S, Leroux M, Mantsch HH. Multianalyte serum analysis using mid-infrared spectroscopy. Ann Clin Biochem 1998 ;35 : 624-632

13. Shaw RA, Kotowich S, Mantsch HH, Leroux M. Quantitation of protein, creatinine, and urea in urine by near-infrared spectroscopy. Clin Biochem 1996 ; 29 : 11-19

14. Hudson L, Poplack FC, Practical immunology, London : Blackwell publication 1976.

15. Holman H-YN, Goth-Goldstein R, Blakely EA, Bjornstad K, Martin MC, Mckinney WR. Individual human cell responses to low doses of chemicals studied by synchrotron Infrered spectromicroscopy. Proceedings of SPIE 2000 ; 3918 : 57-63.

16. Jess P. Acute appendicitis : epidemiology, diagnostics accuracy, and complications. Scnad J Gastroenterol 1983 ; 18 : 161-163.

17. Baldwin AS Jr. The NF-kappa B and I kappa B proteins: new discoveries and insights. Annu Rev Immunol 1996 ;14: 649-683.

18. Lasch P, Naumann D. FT-IR microspectroscopic imaging of human carcinoma thin sections based on pattern recognition techniques. Cell Mol Biol 1998 ; 44 : 189-202.

19. Beebe KR, Pell RJ, Seasholtz MB, Chemometrics : A practical guide New York : Wiley-Interscience, 1998.

20. Salman A, Argov S, Jagannathan Ramesh., Goldstein J, Igor S, Guterman H, Mordechai S. FTIR microscopic characterization of normal and malignant human colonic tissues. Cell. Mol. Biol 2001 ; 47 (22) : OL159-OL166.

21. Garcia-de-Lomas J, Navarro D. New directions in diagnostics Peadiatr Infect Dis J 1997 ; 16 : S43-S48.

22. Whelen AC, Persing DH. The role of nucleic acid amplification and detection in the clinical microbiology laboratory. Annu Rev Microbiol 1996 ; 50 : 349-373.

Figure Captions

Figure 1 : FTIR-MC spectra of blood components of ten representative controls. a) WBC (White Blood Cells) b) RBC (Red Blood cells) c) Plasma in the region 800-1800 cm^{-1}. All the spectra shown in Figures 1-6 were baseline corrected and normalized to amide I band.

Figure 2 : Expanded region of FTIR-MC spectra (900-1500 cm^{-1}) displaying the spectral differences in the symmetric and asymmetric stretching regions of the phosphate group. The spectra are average of ten representative controls. a) WBC b) RBC c) Plasma.

Figure 3 : : FTIR-MC spectra of blood components of ten representative controls. a) WBC b) RBC c) Plasma in the region 2600-3600 cm^{-1}.

Figure 4 : Second derivative spectra of blood components a) WBC (blue) b) RBC (red) c) Plasma (black).

Figure 5 : FTIR-MC spectra of blood components from three age-matched controls (blue) and two acute appendicitis patients (red). a) WBC b) RBC c) Plasma. The inlet

in Figures 4-5 displays an expanded region arising from the symmetric stretching vibrations of phosphate group.

Figure 6 : FTIR-MC spectra of blood components from three age-matched controls (blue) and a patient suffering due to infection in the armpit (axilla). a) WBC b) RBC c) Plasma.

Figure 7 : Dendrogram showing the results obtained from cluster analysis of FTIR-MC spectra of blood components in different regions a) 999-1169 b) 1167-1277 c) 1379-1441 cm^{-1}. Baseline corrected and amide I normalized spectra were used for the cluster analysis. PLS denotes plasma and the number on right side of each blood component represent the control number.

Figure 8 : Dendrogram showing the results obtained from cluster analysis of FTIR-MC spectra of WBC and plasma in different regions a) 945-1282 b) 945-1147 c) 945-1147 cm^{-1}. WBC_SCK denotes the patients suffering due to infection, free WBC stands for age-matched healthy controls and PLS for plasma.

Figure 9 : Dendrogram showing the results obtained from cluster analysis of FTIR-MC spectra of WBC in different regions. a) 945-1282 b) 1146-1282 cm^{-1}. WBC_SCK stands for patient with infection, free WBC for age-matched healthy control and WBC_TST for test cases.

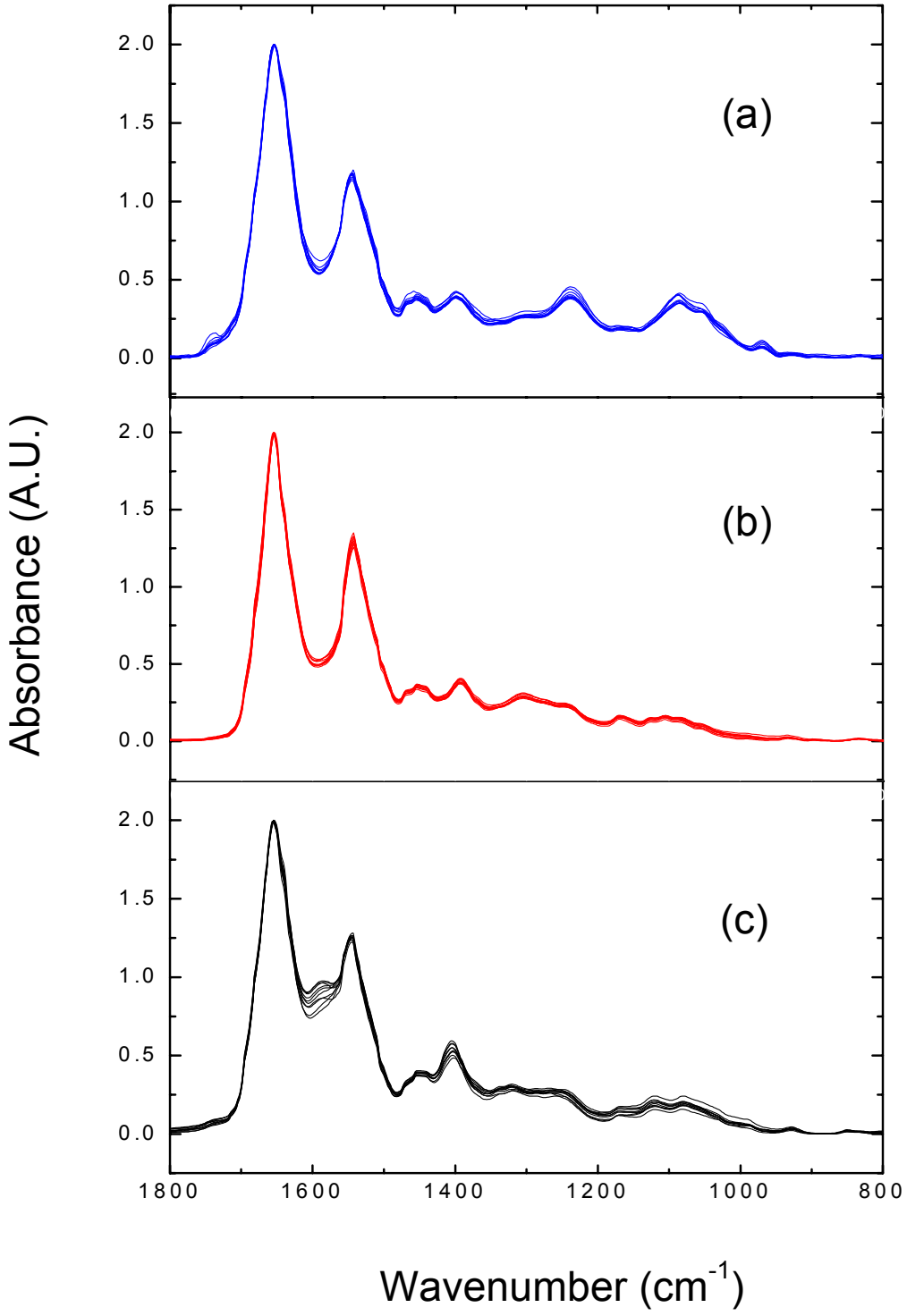
Absorbance (A.U.)
2.0
1.5
1.0
0.5
0.0
(a)
(b)
(c)
1800
1600
1400
1200
1000
800
Wavenumber (cm-1)

figure 1

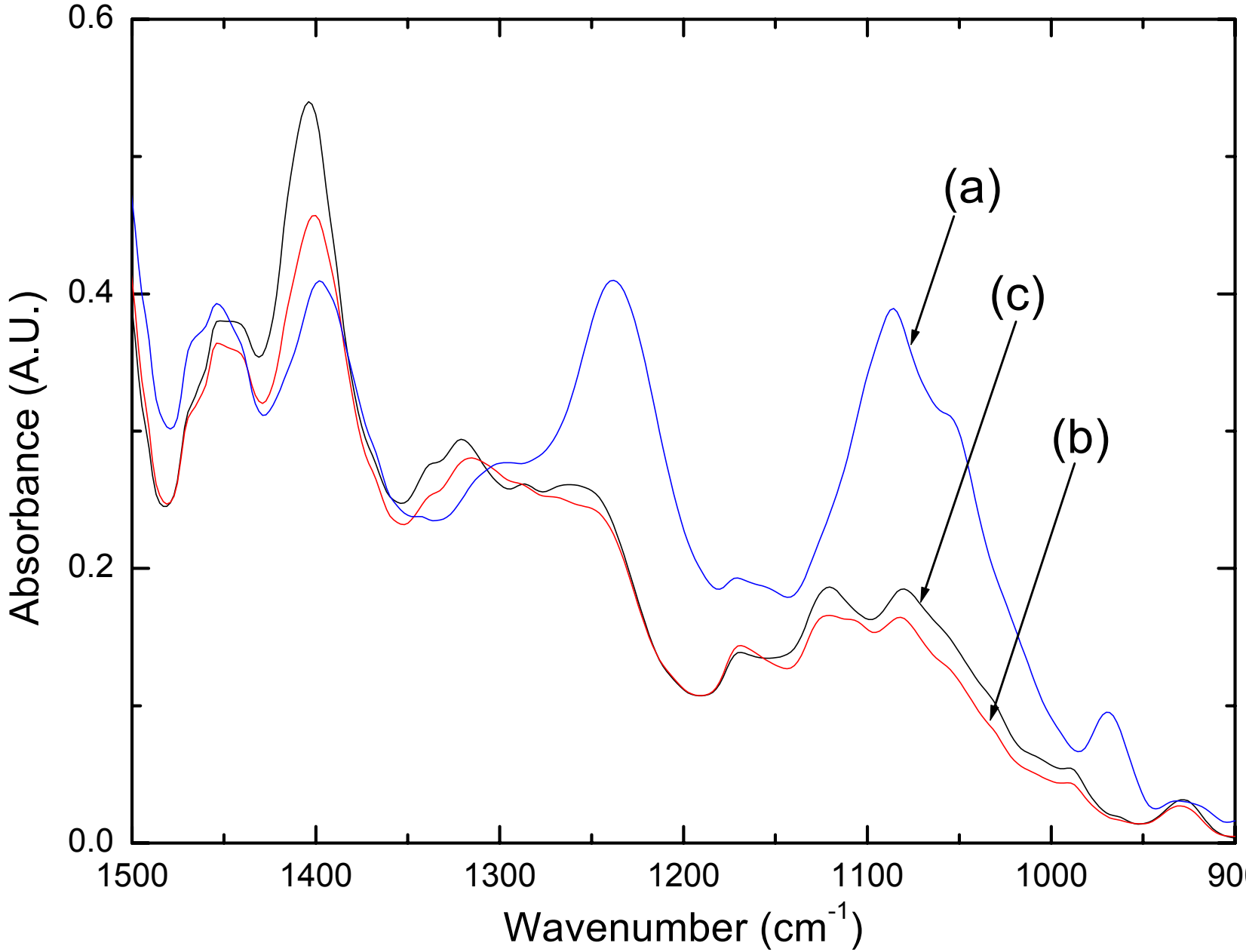
0.6
0.4
0.2
0.0
Absorbance (A.U.)
1500
1400
1300
1200
1100
1000
900
Wavenumber (cm-1)
(a)
(c)
(b)

Figure 2

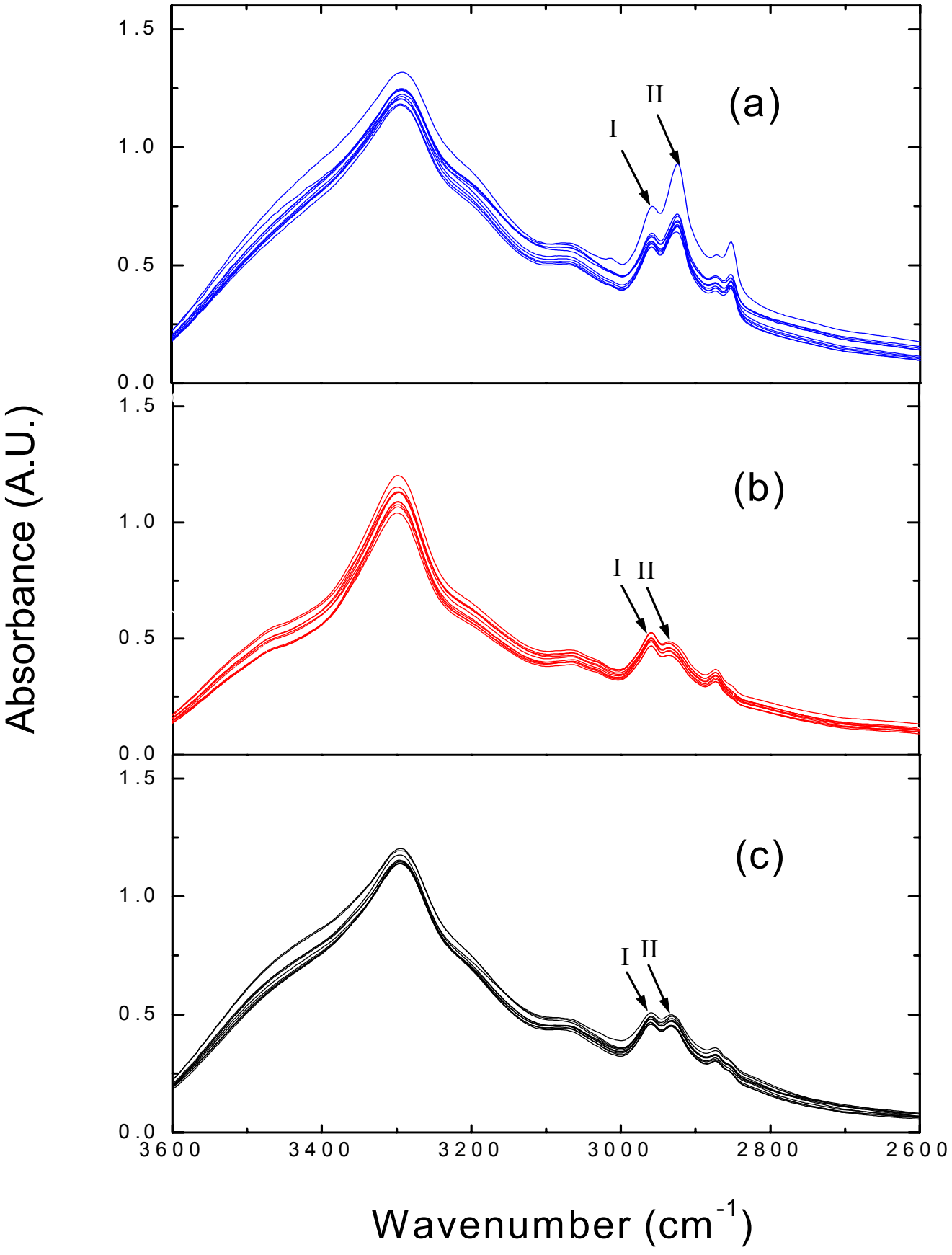
Absorbance (A.U.)
1.5
1.0
0.5
0.0
(a)
I
II
(b)
(c)
3600
3400
3200
3000
2800
2600
Wavenumber (cm-1)

figure 3

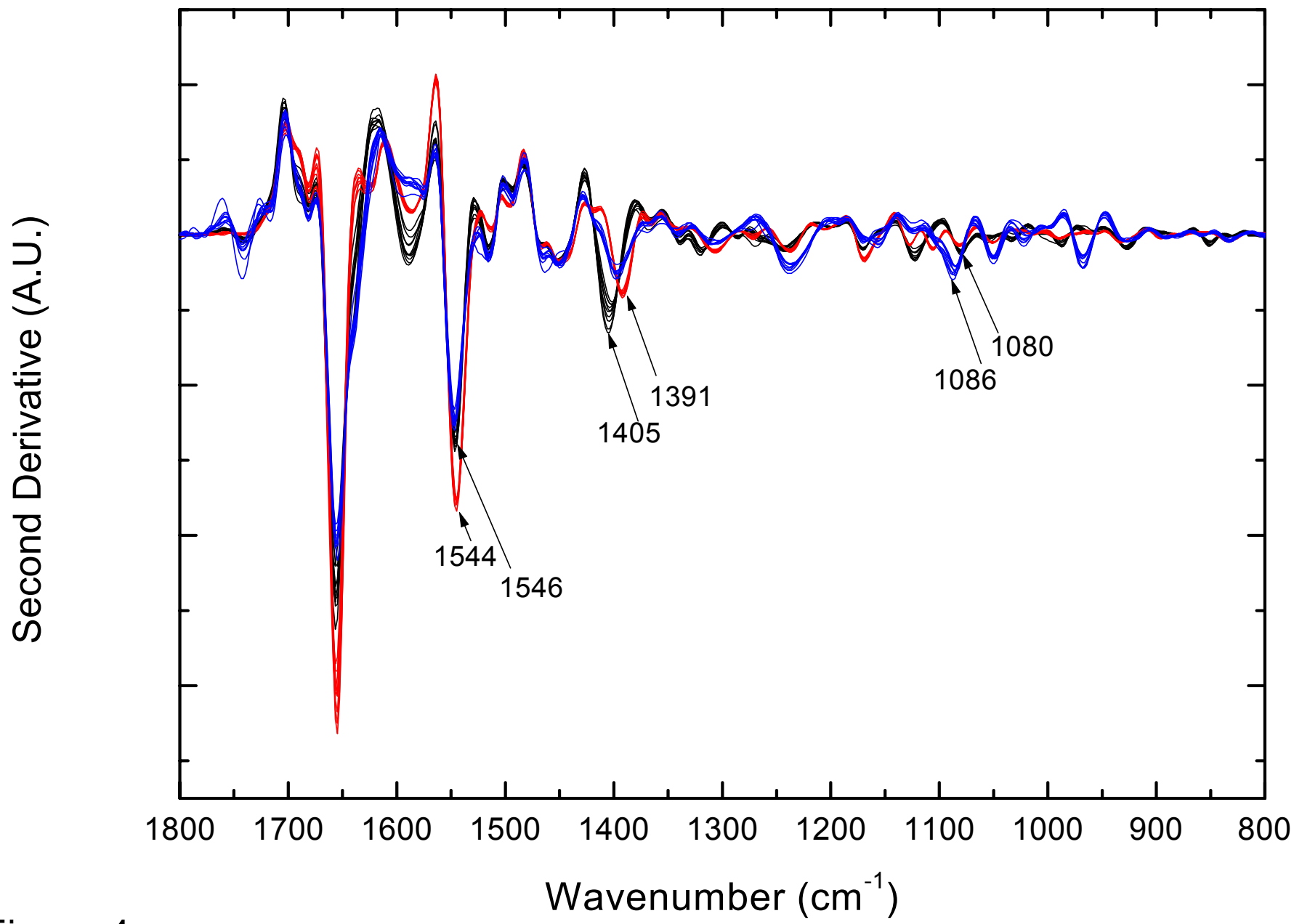
Second Derivative (A.U.)
1800
1700
1600
1500
1400
1300
1200
1100
1000
900
800
Wavenumber (cm-1)
1544
1546
1405
1391
1086
1080

Figure 4

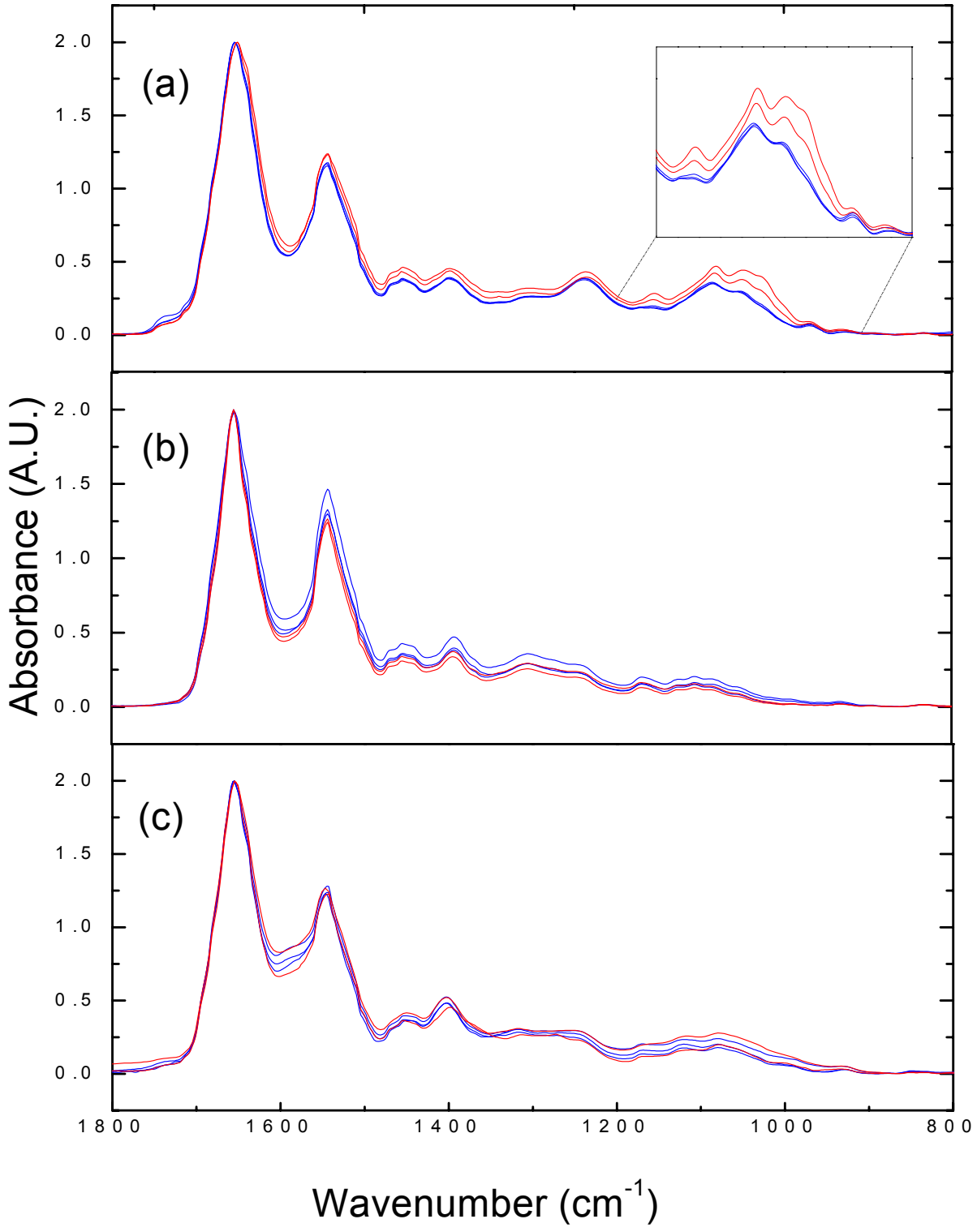
(a)
(b)
(c)
Absorbance (A.U.)
2.0
1.5
1.0
0.5
0.0
1800
1600
1400
1200
1000
800
Wavenumber (cm-1)

figure 5

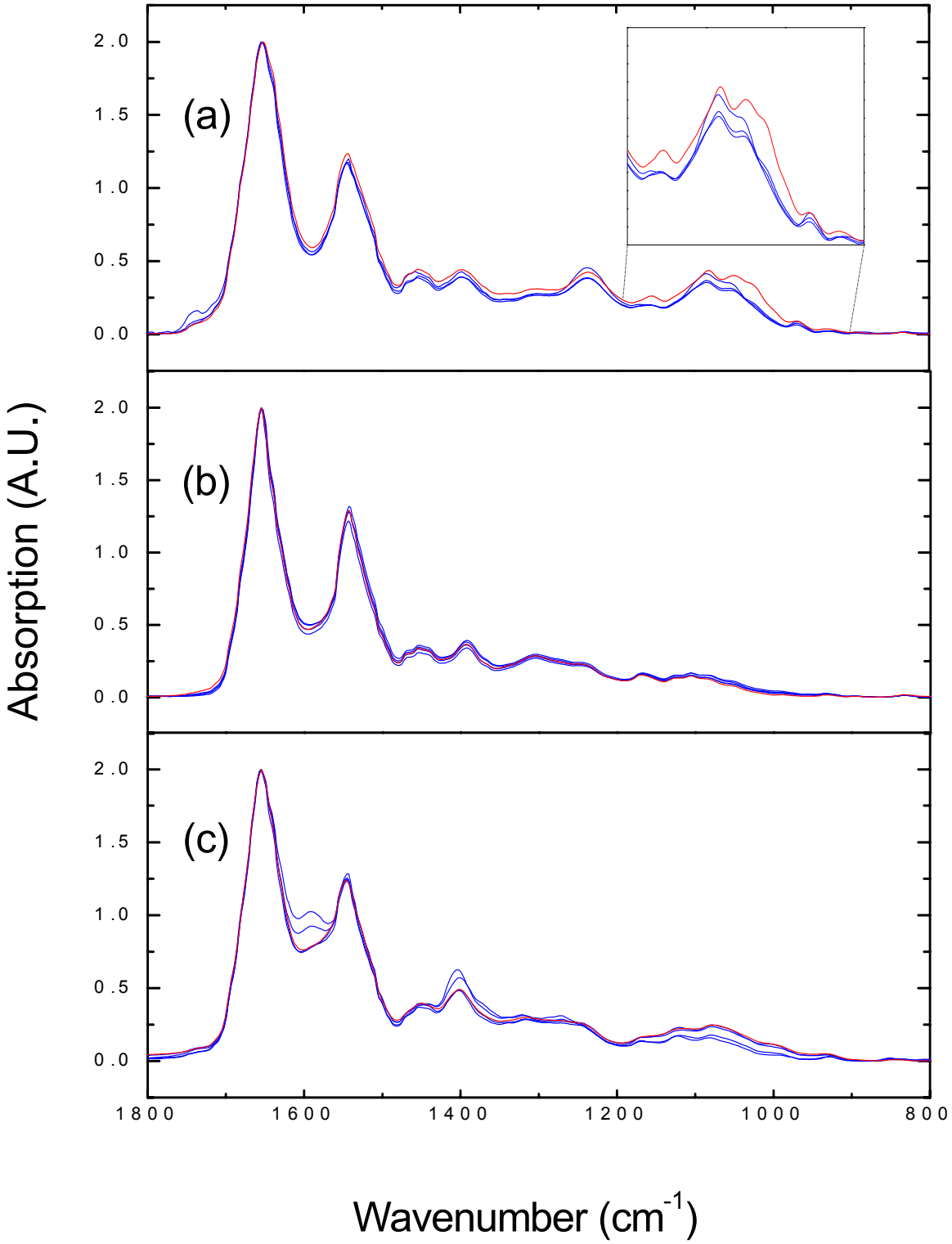
(a)
(b)
(c)
2.0
1.5
1.0
0.5
0.0
1800
1600
1400
1200
1000
800
Absorption (A.U.)
Wavenumber (cm-1)

figure 6

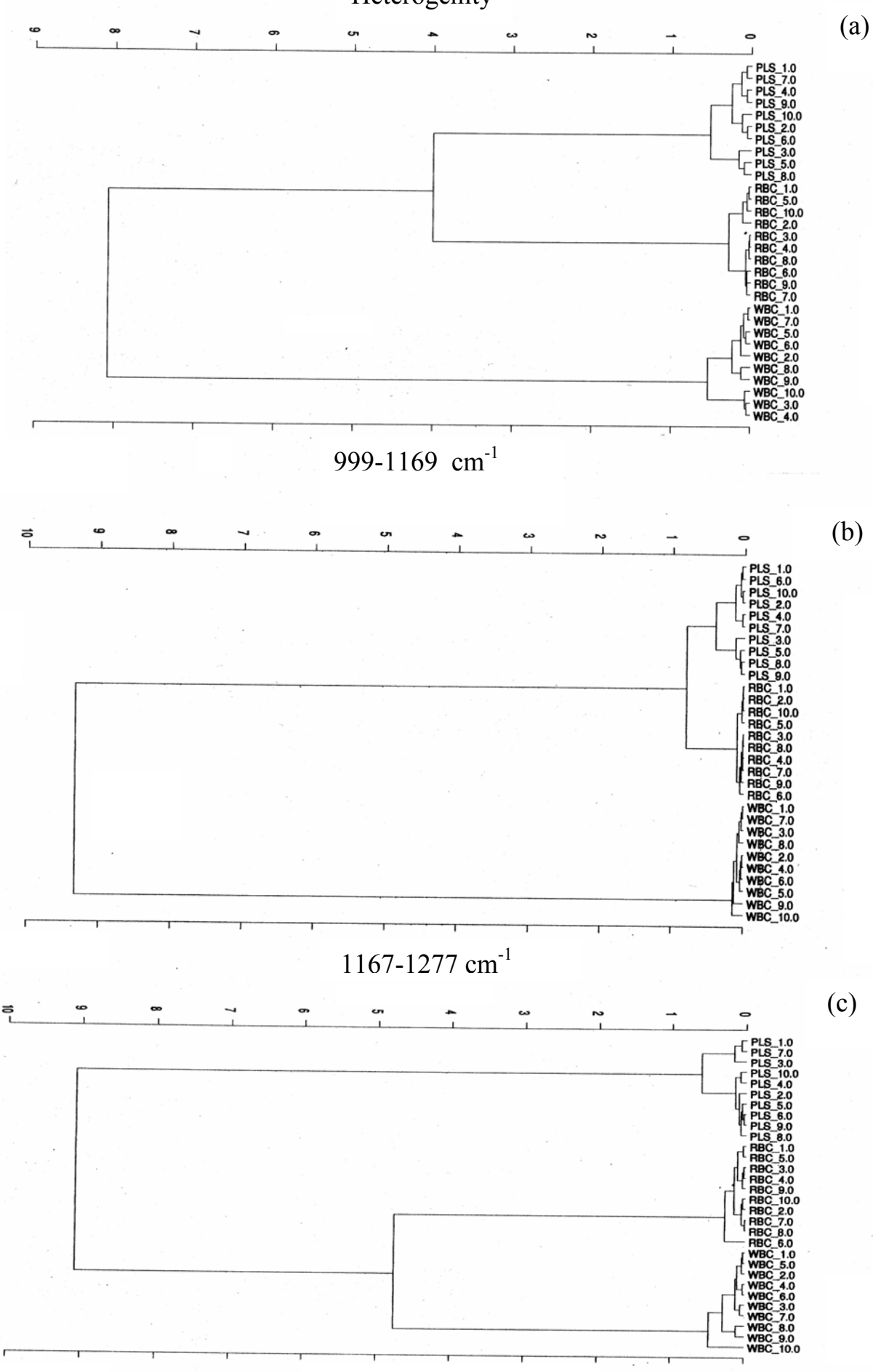
Heterogenity
(a)
9 8 7 6 5 4 3 2 1 0
PLS_1.0
PLS_7.0
PLS_4.0
PLS_9.0
PLS_10.0
PLS_2.0
PLS_6.0
PLS_3.0
PLS_5.0
PLS_8.0
RBC_1.0
RBC_5.0
RBC_10.0
RBC_2.0
RBC_3.0
RBC_4.0
RBC_8.0
RBC_6.0
RBC_9.0
RBC_7.0
WBC_1.0
WBC_7.0
WBC_5.0
WBC_6.0
WBC_2.0
WBC_8.0
WBC_9.0
WBC_10.0
WBC_3.0
WBC_4.0
999-1169 cm-1
(b)
10 9 8 7 6 5 4 3 2 1 0
PLS_1.0
PLS_6.0
PLS_10.0
PLS_2.0
PLS_4.0
PLS_7.0
PLS_3.0
PLS_5.0
PLS_8.0
PLS_9.0
RBC_1.0
RBC_2.0
RBC_10.0
RBC_5.0
RBC_3.0
RBC_8.0
RBC_4.0
RBC_7.0
RBC_9.0
RBC_6.0
WBC_1.0
WBC_7.0
WBC_3.0
WBC_8.0
WBC_2.0
WBC_4.0
WBC_6.0
WBC_5.0
WBC_9.0
WBC_10.0
1167-1277 cm-1
(c)
10 9 8 7 6 5 4 3 2 1 0
PLS_1.0
PLS_7.0
PLS_3.0
PLS_10.0
PLS_4.0
PLS_2.0
PLS_5.0
PLS_6.0
PLS_9.0
PLS_8.0
RBC_1.0
RBC_5.0
RBC_3.0
RBC_4.0
RBC_9.0
RBC_10.0
RBC_2.0
RBC_7.0
RBC_8.0
RBC_6.0
WBC_1.0
WBC_5.0
WBC_2.0
WBC_4.0
WBC_6.0
WBC_3.0
WBC_7.0
WBC_8.0
WBC_9.0
WBC_10.0
1379-1441 cm-1
Frequency Range

Figure 7

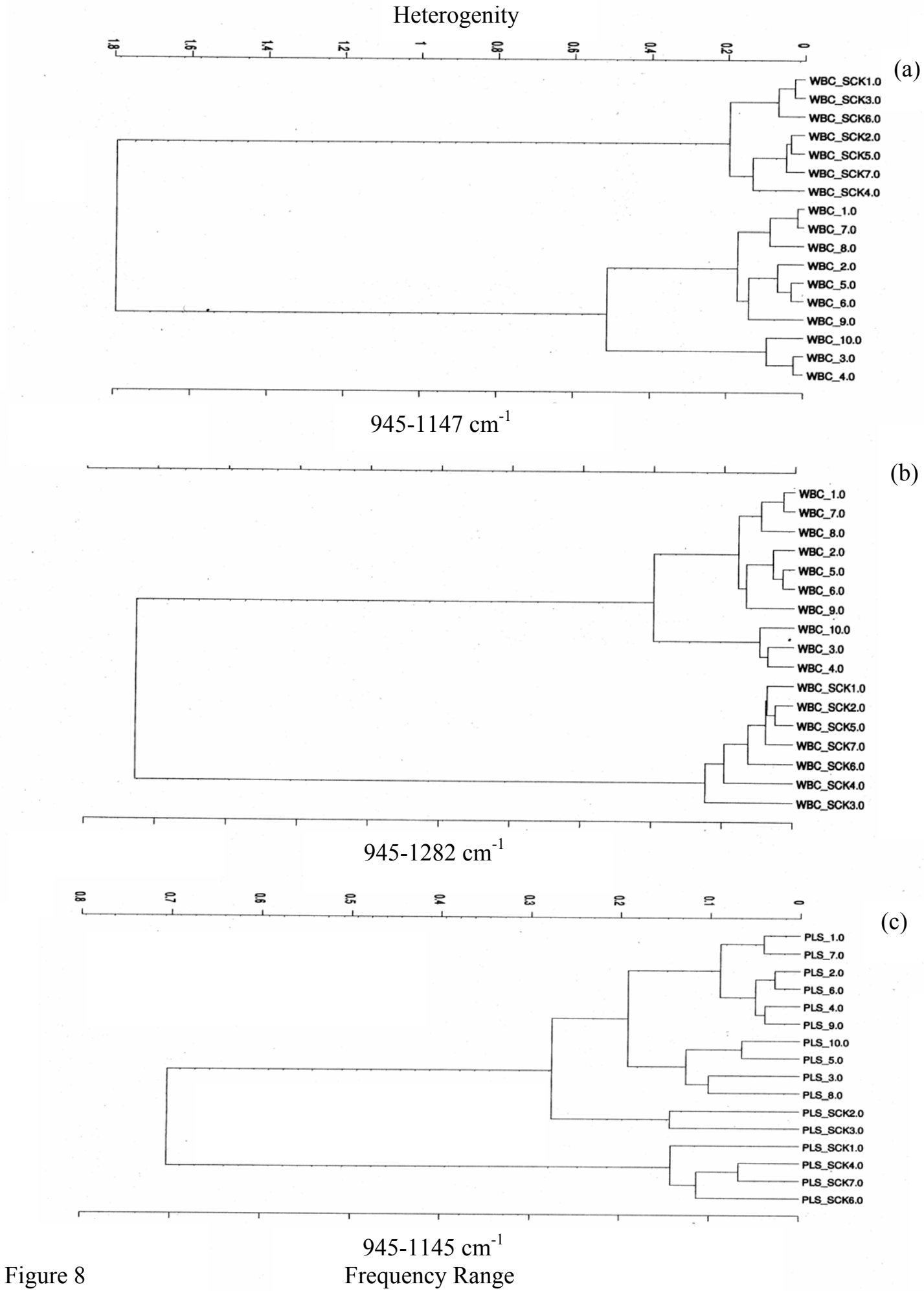
Heterogenity
1.8
1.6
1.4
1.2
1
0.8
0.6
0.4
0.2
0
(a)
WBC_SCK1.0
WBC_SCK3.0
WBC_SCK6.0
WBC_SCK2.0
WBC_SCK5.0
WBC_SCK7.0
WBC_SCK4.0
WBC_1.0
WBC_7.0
WBC_8.0
WBC_2.0
WBC_5.0
WBC_6.0
WBC_9.0
WBC_10.0
WBC_3.0
WBC_4.0
945-1147 cm-1
(b)
WBC_1.0
WBC_7.0
WBC_8.0
WBC_2.0
WBC_5.0
WBC_6.0
WBC_9.0
WBC_10.0
WBC_3.0
WBC_4.0
WBC_SCK1.0
WBC_SCK2.0
WBC_SCK5.0
WBC_SCK7.0
WBC_SCK6.0
WBC_SCK4.0
WBC_SCK3.0
945-1282 cm-1
0.8
0.7
0.6
0.5
0.4
0.3
0.2
0.1
0
(c)
PLS_1.0
PLS_7.0
PLS_2.0
PLS_6.0
PLS_4.0
PLS_9.0
PLS_10.0
PLS_5.0
PLS_3.0
PLS_8.0
PLS_SCK2.0
PLS_SCK3.0
PLS_SCK1.0
PLS_SCK4.0
PLS_SCK7.0
PLS_SCK6.0
945-1145 cm-1
Frequency Range

Figure 8

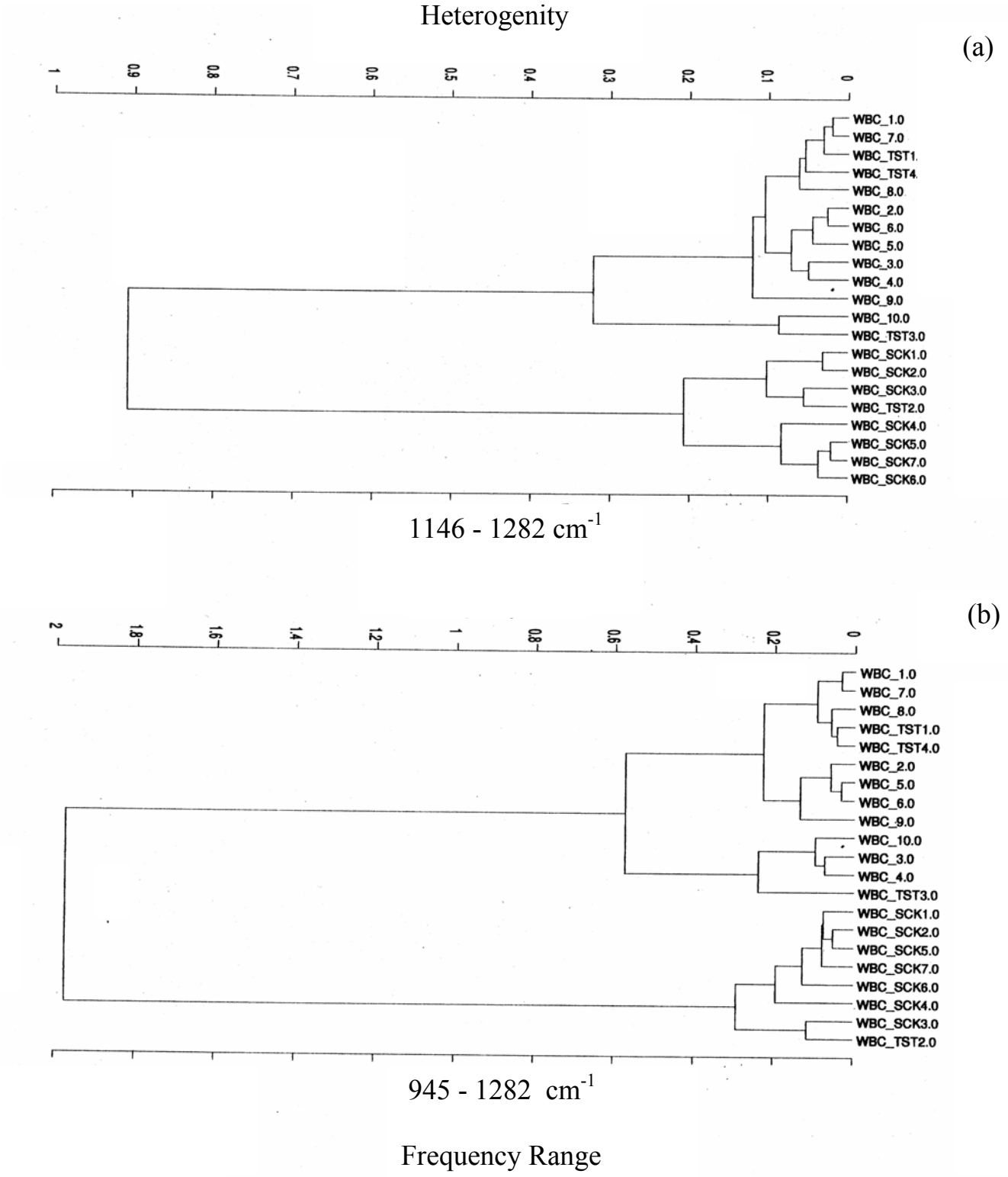
Heterogenity
(a)
1
0.9
0.8
0.7
0.6
0.5
0.4
0.3
0.2
0.1
0
WBC_1.0
WBC_7.0
WBC_TST1.
WBC_TST4.
WBC_8.0
WBC_2.0
WBC_6.0
WBC_5.0
WBC_3.0
WBC_4.0
WBC_9.0
WBC_10.0
WBC_TST3.0
WBC_SCK1.0
WBC_SCK2.0
WBC_SCK3.0
WBC_TST2.0
WBC_SCK4.0
WBC_SCK5.0
WBC_SCK7.0
WBC_SCK6.0
1146 - 1282 cm-1
(b)
2
1.8
1.6
1.4
1.2
1
0.8
0.6
0.4
0.2
0
WBC_1.0
WBC_7.0
WBC_8.0
WBC_TST1.0
WBC_TST4.0
WBC_2.0
WBC_5.0
WBC_6.0
WBC_9.0
WBC_10.0
WBC_3.0
WBC_4.0
WBC_TST3.0
WBC_SCK1.0
WBC_SCK2.0
WBC_SCK5.0
WBC_SCK7.0
WBC_SCK6.0
WBC_SCK4.0
WBC_SCK3.0
WBC_TST2.0
945 - 1282 cm-1
Frequency Range

Figure 9